Optimal Co-Scheduling of HVAC Control and Battery Management for Energy-Efficient Buildings Considering State-of-Health Degradation

Tiansong Cui[1], Shuang Chen[1], Yanzhi Wang[2], Qi Zhu[3], Shahin Nazarian[1] and Massoud Pedram[1]
[1]Department of Electrical Engineering, University of Southern California, USA
[2]Department of Electrical Engineering & Computer Science, Syracuse University, Syracuse, USA
[3]Department of Electrical and Computer Engineering, University of California, Riverside, USA
[1]{tcui, shuangc, shahin, pedram}@usc.edu, [2]ywang393@syr.edu, [3]qzhu@ece.ucr.edu

Abstract— The heating, ventilation and air conditioning (HVAC) system accounts for half of the energy consumption of a typical building. Additionally, the need for HVAC changes over hours and days as does the electric energy price. Level of comfort of the building residents is, however, a primary concern, which tends to overwrite pricing. Dynamic HVAC control under a dynamic energy pricing model while meeting an acceptable level of residents' comfort is thus critical to achieving energy efficiency in buildings in a sustainable manner. The presence of a battery energy storage system in a target building would enable peak power shaving through use of a suitable charge and discharge schedule for the battery, while allowing building energy efficiency and user satisfaction be met. This paper addresses the co-scheduling problem of HVAC control and battery management to achieve energy-efficient buildings, while also accounting for the degradation of the battery state-of-health during charging and discharging operations (which in turn determines the amortized cost of owning and utilizing a battery storage system). A time-of-use dynamic pricing scenario is assumed and various energy loss components are considered including power dissipation in the power conversion circuitry as well as the rate capacity effect in the battery. A global optimization framework targeting the entire billing cycle is presented and an adaptive co-scheduling algorithm is provided to dynamically update the optimal HVAC air flow control and the battery charging/discharging decision in each time slot during the billing cycle to mitigate the prediction error of unknown parameters. Experimental results show that the proposed algorithm achieves up to 15% in the total electric utility cost reduction compared with some baseline methods.

1. INTRODUCTION

The commercial and residential building stock is responsible for 40% of the U.S. primary energy consumption, 40% of the greenhouse gas emissions, and 70% of the electricity use [1]. Among all the energy consumed in buildings, 50% of it is directly related to space heating, cooling, and ventilation [1]. Therefore, reducing building energy consumption by designing smart control mechanism to operate the heating, ventilation and air conditioning (HVAC) system in a more efficient way is critically important to address the nation's energy and environmental concerns. In the literature, various HVAC control mechanisms are proposed to reduce energy cost through storage of thermal energy [2], co-design of HVAC control and embedded platform [3], minimization of total and peak energy consumption using MPC [4], and so on.

Another promising methodology of improving energy efficiency is the adoption of hybrid energy supply in energy-efficient smart buildings, where multiple energy sources are scheduled together to reduce the peak demand and leverage renewable energy sources such as solar radiation [5]. Previous papers have proposed different approaches for efficiently scheduling multiple energy sources [6, 7]. Battery storage is the one of the most popular hybrid energy sources in energy-efficient buildings, because the chemical energy stored inside electrochemical batteries can be converted into electrical energy and delivered to electrical systems whenever and wherever energy is needed [8]. Through proper charging and discharging schedule, the storage ability of batteries is exploited for frequency regulation, load balancing, and peak demand shaving [9, 10, 11].

Although both HVAC control and battery management mechanisms are well researched, there has been little work on formulating the interactions between the two aspects and addressing them together. In the building management system, the demand side scheduling of HVAC control depends on the availability of battery storage and the price of grid electricity, while the supply side scheduling of battery storage requires the knowledge of HVAC demand [5]. As a result, only by addressing these two aspects in an integrated framework can we achieve the maximal energy efficiency in smart buildings. One challenge with battery management in HVAC control system is that it is not clear how much battery aging, and therefore also the associated warranty, are affected during the charging/discharging process. Without a careful consideration of battery aging, the benefits from battery energy storage can hardly be realized in energy-efficient buildings.

To address the above-mentioned issues, we consider the problem of co-scheduling HVAC control and battery management for energy-efficient buildings, aiming to minimize the total cost while maintaining the temperature within the comfort zone for building occupants. In this problem, we explicitly take into account the degradation of battery state-of-health (SoH), which is defined as the ratio of full charge capacity of an aged battery to its designed (nominal) capacity, during the charging and discharging process based on an accurate SoH modeling. We also consider various energy loss components including power dissipation in the power conversion circuitries as well as the rate capacity effect in the battery storage system. In addition, a time-of-use electricity pricing policy is adopted in our model. The objective function to minimize therefore becomes the summation of the building's electricity bill and the extra cost associated with the aging of the battery used in the building energy storage system.

The rest of this paper is organized as follows. We describe our system component models including the building power flow and power conversion, HVAC control system, and battery storage system in Section 2. In Section 3, we provide the formulation and solution of the optimal co-scheduling problem of HVAC control and battery management under the time-of-use electricity pricing policy. Section 4 presents experimental results, and Section 5 concludes the paper.

2. SYSTEM COMPONENT MODELS

In this paper, we consider an energy-efficient smart building with both HVAC control and battery storage systems. Considering that the photovoltaic (PV) system, which converts solar radiation into electricity, is increasingly becoming a key power source and is believed to play an important role in the process of transferring to the future low-carbon power system [12, 13], we consider the building is also equipped with a PV power generation system as well. Our objective is to minimize the combined cost of electricity bill and battery SoH degradation of the building by co-scheduling the air flow of the HVAC control system and the charging/discharging process of the battery storage system.

2.1 Model of Building Power Flow and Power Conversion

The block diagram of the power flow in a typical energy-efficient smart building is shown in Figure 1. The PV system, providing a

power supply of P_{pv}, and the battery storage system, in which the charging power is denoted by P_{bat}, are connected to the building DC power bus through unidirectional and bidirectional DC-DC converters, respectively. Notice that P_{bat} can be positive, negative or zero. A positive value of P_{bat} means the battery is being charged, a negative value indicates discharging from the battery storage, and zero represents no charging or discharging operation. The DC power bus is further connected to the residential AC power bus via bidirectional AC-DC interfaces (e.g., inverters, rectifiers, and transformer circuitries). The power consumption from HVAC control system (P_{hvac}) is the part that we need to manage in this paper. The building AC load on the AC bus (P_{load}) corresponds to other building tasks such as lighting, fire and security. The AC power bus is further connected to the state-level or national smart grid and the power from the grid P_{grid} is related to the building's electricity bill. We consider realistic power conversion circuits (i.e., the power conversion efficiency is less than 100%) in this work, and use η_1, η_2 and η_3 to denote the power efficiency of the converters between the PV system and the DC power bus, the converters between the battery storage and the DC power bus, and the AC-DC interface connecting the DC power bus and the AC power bus, respectively. Typical conversion efficiency values are in the range of 85% to 95% [14, 15]. There are three *operation modes*

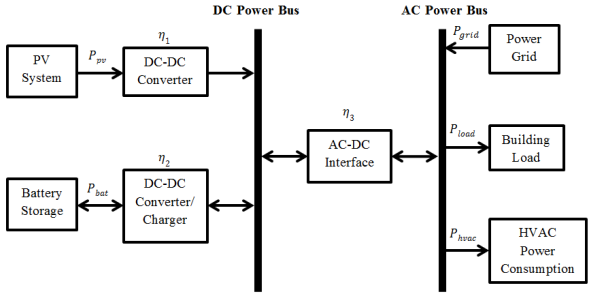

Figure 1: Power flow of an energy-efficient smart building including HVAC control, PV system, battery storage system, building load and the external power grid. The directions of arrows represent the directions of the power flow.

in the above-mentioned power flow. In the first mode, the battery system is discharging ($P_{bat} \leq 0$), and thus, the building loads are supplied simultaneously by the grid, the PV system as well as the battery storage. In the second mode, the battery system is charged by the PV system only, and the surplus PV power generation is used to supply HVAC system and other building loads. In this mode, part of the power generated by the PV system flows from the DC bus to the AC bus ($\eta_1 \cdot P_{pv} - \frac{1}{\eta_2} \cdot P_{bat} \geq 0$). In the last mode, the PV system is not sufficient for charging the battery storage ($\eta_1 \cdot P_{pv} - \frac{1}{\eta_2} \cdot P_{bat} < 0$). Thus, the battery storage is simultaneously charged by the PV system as well as the converted power from grid. In general, P_{grid} can be calculated using the following equation:

$$P_{grid} = \begin{cases} P_{hvac} + P_{load} - \eta_3(\eta_1 P_{pv} - \eta_2 P_{bat}), & P_{bat} \leq 0 \\ P_{hvac} + P_{load} - \eta_3(\eta_1 P_{pv} - \frac{1}{\eta_2} P_{bat}), & 0 < P_{bat} \leq \eta_1 \eta_2 P_{pv} \\ P_{hvac} + P_{load} - \frac{1}{\eta_3}(\eta_1 P_{pv} - \frac{1}{\eta_2} P_{bat}), & P_{bat} > \eta_1 \eta_2 P_{pv} \end{cases} \quad (1)$$

For the convenience of expression, the relationship in Eqn. (1) will be referred to as $P_{grid} = f_{grid}(P_{hvac}, P_{load}, P_{pv}, P_{bat})$ in the rest of this paper.

2.2 Model of HVAC control

HVAC is the technology of indoor and vehicular environmental which aims at providing thermal comfort and acceptable indoor air quality. Previous work [16] used an encoded temperature variable $T_{ctrl}(t)$ and $u(t)$ to represent the room temperature state and air flow at a certain time t. Assuming the HVAC system keeps an air flow $u(t)$ for a certain time period Δ_t, the room temperature updates following the equation:

$$T_{ctrl}(t + \Delta_t) = A_n \cdot T_{ctrl}(t) + B_n \cdot u(t) + E_n \cdot D(t), \quad (2)$$

where A_n, B_n and E_n are HVAC specific parameters which are functions of Δ_t, $T_{ctrl}(t)$ is a state vector comprised of five elements, and $D(t)$ is the disturbance from external sources (e.g. solar radiance, wind, etc.) at time t. The five elements in $T_{ctrl}(t)$ correspond to the temperature of the four surrounding walls of a room and the temperature of the room itself. To maintain the building temperature at a comfortable zone, at any time t, $T_{ctrl}(t)$ needs to satisfy the following constraint:

$$T_{lowBound}(t) \leq C_n \cdot T_{ctrl}(t) \leq T_{upBound}(t), \quad (3)$$

where $C_n = [0\ 0\ 0\ 0\ 1]$ is used to find the temperature of the room, and $T_{lowBound}(t)$ and $T_{upBound}(t)$ are the lower bound and upper bound of the comfort zone in terms of air termperature at a certain time. The air flow also needs to follow the constraint:

$$U_{lowBound} \leq u(t) \leq U_{upBound}, \quad (4)$$

meaning that the maximal achievable value of $u(t)$ is $U_{upBound}$, while the minimal achievable value of $u(t)$ is $U_{lowBound}$. Given the HVAC air flow, its power consumption P_{hvac} can be calculated using the equation:

$$P_{hvac}(t) = (c_1 \cdot u(t)^3 + c_2 \cdot u(t)^2 c_3 \cdot u(t) + c_4) AC_p / 100 \quad (5)$$

where c_1, c_2, c_3 and c_4 are HVAC power coefficients [16] and AC_p represents the AC power in the system.

2.3 Model of Battery System

2.3.1 Battery Storage

The most critical effect that causes power loss in the storage system of a battery is the rate capacity effect [17]. High-peak pulsed discharging current will deplete much more of the battery's stored energy than a smooth workload with the same total energy demand. We define *discharging efficiency* of a battery, denoted by $\eta_{rate,d}$, as the ratio of the battery's output current to the degradation rate of its stored charge amount. The rate capacity effect specifies that the discharging efficiency of a battery decreases with the increase of the battery's discharging current. The *charging efficiency* of a battery, denoted by $\eta_{rate,c}$, is defined similarly.

According to Peukert's formulae [18], $\eta_{rate,d}$ and $\eta_{rate,c}$ are described as functions of the charging current I_c and the discharging current I_d, respectively, as follows:

$$\eta_{rate,c}(I_c) = \frac{1}{(I_c/I_{ref})^{\alpha_c}}, \ \eta_{rate,d}(I_d) = \frac{1}{(I_d/I_{ref})^{\alpha_d}} \quad (6)$$

where α_c and α_d are Peukert's coefficients with typical values in the range of 0.1-0.3, I_{ref} denotes the reference current level for charging and discharging which is typically the current that can fully deplete the battery in 20 hours. It can be observed that the efficiency values $\eta_{rate,c}$ and $\eta_{rate,d}$ in Eqn. (6) will be higher than 100% if $I_c < I_{ref}$ or $I_d < I_{ref}$, which contradicts common sense. To address this issue, we use a slightly modified version of Peukert's formulae such that $\eta_{rate,c}$ and $\eta_{rate,d}$ will be saturated at 100% when the charging/discharging current is low.

We denote the change rate of the stored energy in the battery by $P_{bat,int}$, which can be positive (charging the storage), negative (discharging from the storage), or zero. Based on the modified Peukert's formulae, the relationship between $P_{bat,int}$ and the input power of the battery, denoted by P_{bat}, is given by

$$P_{bat} = \begin{cases} V_{bat} \cdot I_{bat,ref} \cdot (\frac{P_{bat,int}}{V_{bat} \cdot I_{bat,ref}})^{\beta_c}, & \frac{P_{bat,int}}{V_{bat} \cdot I_{bat,ref}} > 1 \\ -V_{bat} \cdot I_{bat,ref} \cdot (\frac{|P_{bat,int}|}{V_{bat} \cdot I_{bat,ref}})^{\beta_d}, & \frac{P_{bat,int}}{V_{bat} \cdot I_{bat,ref}} < -1 \\ P_{bat,int}, & otherwise \end{cases} \quad (7)$$

where V_{bat} is the battery terminal voltage and is assumed to be (nearly) constant, and coefficients β_c and β_d are given by

$$\beta_c = \frac{1}{1 - \alpha_c}, \ \beta_d = \frac{1}{1 + \alpha_d} \quad (8)$$

For the convenience of expression, the relationship in Eqn. (7) will be referred to as $P_{bat} = f_{bat}(P_{bat,int})$ in the rest of this paper. One important observation is that this function is a convex and monotonically increasing function over the input domain $-\infty < P_{bat,int} < \infty$. An example of $f_{bat}(\cdot)$ with $\beta_c = 1.1$ and $\beta_d = 0.9$ is shown in Figure 2, from which one can see that rate capacity effect makes the charging/discharging process less efficient.

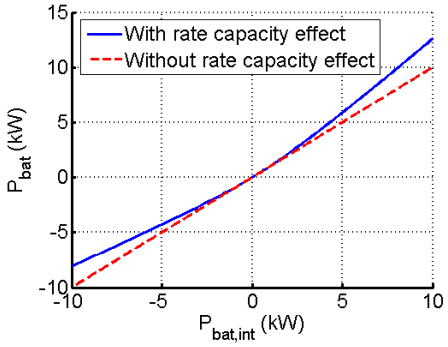

Figure 2: Relationship between P_{bat} and $P_{bat,int}$ considering the rate capacity effect.

2.3.2 *Battery SoH Degradation*

Another significant portion of power loss for batteries [19] is due to the state-of-health (SoH) degradation, i.e. the charge capacity of a battery will slowly degrade as the battery ages. The amount of SoH degradation, denoted by D_{SoH}, is defined as:

$$D_{SoH} = \frac{C_{full}^{nom} - C_{full}}{C_{full}^{nom}} \times 100\% \tag{9}$$

where C_{full}^{nom} is the nominal charge capacity of a new battery and C_{full} is the charge capacity of the battery in its current state. Considering the SoH degradation, the state-of-charge (SoC) of a battery is defined as follows:

$$SoC = \frac{C_{bat}}{C_{full}} \times 100\% \tag{10}$$

where C_{bat} is the remaining charge stored in the battery. The SoH degradation of a battery is difficult to estimate because it is related to a set of long-term electrochemical reactions inside the battery. These effects strongly depend on the operating condition of the battery such as charging and discharging currents, number of charge-discharge cycles, SoC swing, average SoC, and operation temperature [20, 21]. Although very accurate, some electrochemistry-based models such as the one proposed in [22] are too complicated to be applied to an optimization problem like ours. In this paper, we use the SoH degradation model proposed in [23], which calculates the SoH degradation based on charging cycles and shows a good match with real data. In the applied model, a *charging cycle* is defined as a process of charging a battery cell from SoC_{low} to SoC_{high} and discharging it from SoC_{high} to SoC_{low} after that. The average SoC and the SoC swing during one charging cycle, denoted by SoC_{avg} and SoC_{swing}, respectively, are defined as follows:

$$SoC_{avg} = (SoC_{low} + SoC_{high})/2 \tag{11}$$

$$SoC_{swing} = SoC_{high} - SoC_{low} \tag{12}$$

The SoH degradation of one charging cycle, denoted by $D_{SoH,cycle}$, is calculated as

$$\begin{aligned} D_1 &= K_{CO} \cdot exp[(SoC_{swing} - 1) \cdot \frac{T_{ref}}{K_{ex} \cdot T_B}] + 0.2\frac{\tau}{\tau_{life}} \\ D_2 &= D_1 \cdot exp[4K_{SoC} \cdot (SoC_{avg} - 0.5)] \cdot (1 - D_{SoH}) \\ D_{SoH,cycle} &= D_2 \cdot exp[K_T \cdot (T_B - T_{ref}) \cdot \frac{T_{ref}}{T_B}] \end{aligned} \tag{13}$$

where K_{co}, K_{ex}, K_{SoC}, and K_T are battery specific parameters; T_B and T_{ref} are the battery's operation temperature and reference temperature, respectively, τ is the duration of this charging/discharging cycle, and τ_{life} is the calendar life of this battery.

We use $D_{SoH,cycle}(SoC_{swing}, SoC_{avg})$ to denote the relationship between $D_{SoH,cycle}$, SoC_{swing}, and SoC_{avg}. The total SoH degradation (compared to a new battery) after M charging cycles is calculated by:

$$D_{SoH} = \sum_{m=1}^{M} D_{SoH,cycle,m} \tag{14}$$

where $D_{SoH,cycle,m}$ denotes the SoH degradation in the m-th cycle calculated using Eqn. (13). One can observe in Eqn. (13) that the normalized SoH degradation value D_{SoH} accumulates over the battery lifetime from 0 (brand new) to 100% (no capacity left). In the literature, one typically uses $D_{SoH} = 20\%$ or $D_{SoH} = 30\%$ as a threshold to indicate the battery's end of life. An example of SoH degradation under different SoC_{avg}'s and SoC_{swing}'s with a threshold of $D_{SoH} = 20\%$ is shown in Figure 3. There are two important observations drawn from the figure: (i) a higher SoH degradation rate is caused by both a higher SoC swing and a higher average SoC level in each charging/discharging cycle, and (ii) the cycle life of a Li-ion battery increases superlinearly with respect to the reduction of SoC swing and average SoC.

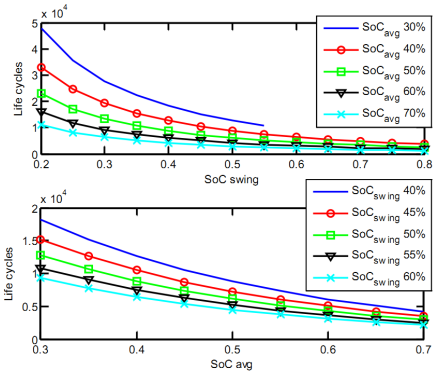

Figure 3: Li-ion battery SoH degradation versus SoC swing (at different average SoC levels) and average SoC level (at different SoC swings).

3. HVAC CONTROL AND BATTERY MANAGEMENT CO-SCHEDULING ALGORITHM

3.1 Problem description

In this section, we present the formulation and solution of the cost minimization problem for an energy-efficient building through the co-scheduling of HVAC control and battery management. A slotted time model is adopted for decision making in which all system constraints as well as decisions are provided for discrete time intervals with equal and constant length Δ_t, and we consider the optimization framework for a *billing period* with N time slots. The temperature variable in HVAC system and battery SoC level at time slot i are denoted by $Tctrl[i]$ and $SoC[i]$ respectively where $0 \leq i \leq N$. The initial building temperature variable is given by $Tctrl[0] = Tctrl_{ini}$, the initial SoC level of the battery is given by $SoC[0] = SoC_{ini}$. We assume the battery can be re-used in the next billing cycle, the final SoC level $SoC[N]$ should also be SoC_{ini}. The total cost function is comprised of two parts: the energy cost charged from the power grid, and the cost associated with battery aging, given as follows:

$$Cost_{total} = Cost_{energy} + Cost_{aging} \tag{15}$$

We consider a dynamic pricing function is offered by the power grid, in which the price of one unit of energy (kWh) during the i-th time slot is denoted by $\Pi[i]$ and is pre-announced at the beginning of the

billing period. The energy cost in Eqn. (15) is calculated as follows:

$$Cost_{energy} = \sum_{i=1}^{N} \Pi[i] \cdot P_{grid}[i] \cdot \Delta_t \quad (16)$$

And the battery aging cost is given by (we assume that the battery reaches end-of-life when SoH degradation is 30%):

$$Cost_{aging} = \frac{D_{SoH}}{1 - SoH_{th}} \cdot Cost_{bat} \quad (17)$$

where $Cost_{bat}$ is the cost to purchase and replace the battery, D_{SoH} represents the amount of SoH degradation during the charging and discharging process, and SoH_{th} is the threshold SoH level (typically 70%) at which the battery should be replaced.

According to Eqn. (1), $P_{grid}[i]$ is a function of battery charging, PV power generation, building power load as well as HVAC power consumption (denoted by $P_{bat}[i]$, $P_{pv}[i]$, $P_{load}[i]$, and $P_{hvac}[i]$ respectively) at time slot i. Apart from $P_{hvac}[i]$ and $P_{bat}[i]$ which can be controlled by HVAC and battery systems, the values of $P_{pv}[i]$ and $P_{load}[i]$ can not be exactly determined until time slot i unfolds. In order to reflect the potential opportunity for peak power shaving through co-scheduling of HVAC control and battery management in all future time slots, we propose to estimate the values of $P_{pv}[i]$ and $P_{load}[i]$ (denoted by $\hat{P}_{pv}[i]$ and $\hat{P}_{load}[i]$) based on other factors such as weather report, building task schedule, and data from history.

However, the prediction error of these parameters adds to the difficulty of accurately calculating the total cost while maintaining certain constrains in future time slots. To tackle this problem, we propose the following adaptive co-scheduling framework to handle the prediction error. At the beginning of the i-th time slot, the HVAC power consumption and battery charging plan are determined for all future time slots based on the current knowledge of the system parameters (either given or estimated). While the actions of $P_{hvac}[i]$ and $P_{bat}[i]$ take place at the i-th time slot, the values of $P_{hvac}[i+1], \ldots, P_{hvac}[N]$ and $P_{bat}[i+1], \ldots, P_{bat}[N]$ will be further updated at the next decision epoch at the beginning of the $(i+1)$-th time slot when our knowledge of parameters including $\hat{P}_{pv}[i+1]$ and $\hat{P}_{load}[i+1]$ are updated.

3.2 Adaptive Co-Scheduling Problem Formulation

We describe the adaptive co-scheduling problem of HVAC control and battery management at the beginning of the i-th hour. At that time, the current temperature variable and the SoC level of the battery is given by $T_{ctrl}[i-1]$ and $SoC[i-1]$. The amount of HVAC power consumption and battery charging, i.e. $P_{hvac}[i]$ and $P_{bat}[i]$, are derived by jointly considering the next hour (the i-th hour) and all other hours in the future (the $(i+1)$-th to N-th hour). As mentioned in Section 3.1, in order to consider all future time slots, the unknown parameters including the PV power generation and building power load will first be estimated. While finding these estimations, we assume that necessary information (e.g. weather report, building task schedule, data from history, etc.) is available.

To estimate the future building temperature change under a certain level of HVAC power consumption, we first need to determine the air flow at the that time slot. According to Eqn. (5), relationship between $P_{hvac}[i']$ and the air flow at a future time slot i' (denoted by $u[i'], i \le i' \le N$) is given by:

$$P_{hvac}[i'] = (c_1 \cdot u[i']^3 + c_2 \cdot u[i']^2 + c_3 \cdot u[i'] + c_4) AC_p/100 \quad (18)$$

For the convenience of expression, the relationship in Eqn. (18) will be referred to as $P_{havc}[i'] = f_{hvac}(u[i'])$ in the rest of this paper. Notice that $u[i']$ and $P_{hvac}[i']$ have a one-to-one mapping relationship. To solve the problem more effectively, we set $u[i']$ as our optimization variable in our algorithm.

And based on Eqn. (2), estimated temperature variable will update at time slot i' following the equation:

$$\hat{T}_{ctrl}[i'] = A_n \cdot \hat{T}_{ctrl}[i'-1] + B_n \cdot u[i'] + E_n \cdot \hat{D}[i'], i \le i' \le N \quad (19)$$

where A_n, B_n and E_n are HVAC specific parameters corresponding to Δ_t and $\hat{D}[i']$ is another estimated value which should be predicted and dynamically updated based on the most recent information.

In addition, SoC values for future time slots, denoted by $SoC[i']$, are determined by:

$$SoC[i'] = SoC[i-1] + \sum_{j=i}^{i'} \frac{P_{bat,int}[j] \cdot \Delta_T}{V_{bat} \cdot C_{full}}, i \le i' \le N \quad (20)$$

where $P_{bat,int}[j]$ is a function of $P_{bat}[j]$ and can be calculated according to Eqn. (7). Considering that there is also a one-to-one mapping relationship between $P_{bat,int}[j]$ and $P_{bat}[j]$ and we set $P_{bat,int}[j]$ as our optimization variable in our algorithm.

Knowing the SoC values of future time slots, we provide as follows an estimate of the SoH degradation of the battery during the charging and discharging process. We approximate the combination of the process as multiple charge/discharge cycles of the battery in all the future time slots. The highest and lowest SoC values $SoC_{high}[i]$ and $SoC_{low}[i]$ in these discharge/charge cycles are:

$$SoC_{high}[i] = \max_{i \le i' \le N} SoC[i'] \quad (21)$$

$$SoC_{low}[i] = \min_{i \le i' \le N} SoC[i'] \quad (22)$$

And the SoH degradation of the battery in future time slots is estimated by:

$$D_{SoH}[i] = N_C[i] \cdot D_{SoH,cycle}(SoC_{swing}[i], SoC_{avg}[i]) \quad (23)$$

where $D_{SoH,cycle}(SoC_{swing}[i], SoC_{avg}[i])$ is defined as in Eqn. (13) and $N_C[i]$ is the equivalent charging cycles in future time slots that can be calculated as

$$N_C[i] = \sum_{j=i}^{N} \frac{P_{bat,int}[j] \cdot \mathbf{I}[P_{bat}[j] > 0] \cdot \Delta_t}{V_{bat} \cdot C_{full} \cdot SoC_{swing}} \quad (24)$$

where $\mathbf{I}$[-] is the indicator function. Based on the above calculations, the adaptive control problem at the beginning of time slot i ($1 \le i \le N$) can be formulated as follows:

Given: Current SoC level $SoC[i-1]$, current temperature condition $T_{ctrl}[i-1]$.

Predict: $\hat{P}_{pv}[i']$, $\hat{P}_{load}[i']$ and $\hat{D}[i']$ for $i \le i' \le N$.

Find: $u[i']$ and $P_{bat,int}[i']$ for $i \le i' \le N$.

Minimize: Estimated objective function in Eqn.(15).

Subject to: HVAC temperature constraint, HVAC air flow constraint, battery charging constraint, and battery SoC constraint.

To solve the problem efficiently after predicting the values of the unknown parameters, we propose to use a solution framework with an outer loop and a kernel algorithm. In the outer loop, we iterate over a set of possible values of $SoC_{high}[i]$ and $SoC_{low}[i]$. In each iteration, given the range of the SoC of the battery during the charging and discharging process, we formulate an optimization problem as follows:

Find: $u[i']$'s and $P_{bat,int}[i']$'s.

Minimize:

$$\sum_{i'=i}^{N} \Pi[i'] \cdot P_{grid}[i'] \cdot \Delta_t + \frac{D_{SoH}[i]}{1 - SoH_{th}} \cdot Cost_{bat} \quad (25)$$

Subject to:

$$P_{grid}[i'] = f_{grid}(P_{hvac}[i'], \hat{P}_{load}[i'], \hat{P}_{pv}[i'], P_{bat}[i']), \forall i' \quad (26)$$

$$C_n \cdot \hat{T}_{ctrl}[i'] \geq T_{lowBound}[i'] + \sigma, \forall i' \quad (27)$$

$$C_n \cdot \hat{T}_{ctrl}[i'] \leq T_{upBound}[i'] - \sigma, \forall i' \quad (28)$$

$$P_{hvac}[i'] = f_{hvac}(u[i']), \forall i' \quad (29)$$

$$U_{lowBound} \leq u[i'] \leq U_{upBound}, \forall i' \quad (30)$$

$$P_{bat}[i'] = f_{bat}(P_{bat,int}[i']), \forall i' \quad (31)$$

$$-P_{bat,max,D} \leq P_{bat}[i'] \leq P_{bat,max,C}, \forall i' \quad (32)$$

$$SoC[i'] = SoC[i-1] + \sum_{j=i}^{i'} \frac{P_{bat,int}[j] \cdot \Delta_T}{V_{bat} \cdot C_{full}}, \forall i' \quad (33)$$

$$SoC[N] \geq SoC_{ini} \quad (34)$$

$$SoC_{low} \leq SoC[i'] \leq SoC_{high}, \forall i' \quad (35)$$

Eqn. (26) is the relationship in the system power flow. Eqn. (27)-(30) are HVAC related constraints. Constraints (27) and (28) ensure that the building stays at comfortable temperature zone. Notice that σ is a parameter that accounts for the prediction error of $\hat{D}[i']$, and can be set proportional to $T_{upBound}[i'] - T_{lowBound}[i']$. Constraint (29) captures the relationship between the HVAC air flow and HVAC power consumption and constraint (29) sets air flow upper bound and lower bound. Eqn. (31)-(35) are battery related constraints. Constraint (31) captures the relation between the input power from the DC bus and the energy change inside the battery. Constraint (32) sets the bounds for the total charging and discharging power of the battery. Constraint (33) calculates the SoC level of the battery for each future time slot. Constraint (34) ensures that the SoC reaches at least the initial SOC level at the end of the billing cycle. And constraint (35) ensures that the SoC of the battery will not go beyond the SoC bound set in the outer loop in future time slots.

In order to solve the kernel optimization problem, we first eliminate constraints (31) and (26) by substituting P_{bat} in Eqn. (26) using (31) and substitute P_{grid} in the objective function using Eqn. (26). Then all the inequality constraints are convex and all the remaining equality constraints are affine. As mentioned in Section 2.3.1, f_{bat} is a convex function. Noticing that usually we have $c_1 < 0$, $c_2 > 0$, and $c_1 \ll c_2$(an example can be found in [16]), it can also be proved that $P_{havc}[i']$ in Eqn. (18) is a convex function of $u[i']$ when $u[i'] \leq \frac{c_2}{3c_1}$. Therefore, we can set $\frac{c_2}{3c_1}$ as an additional upper bound for $u[i']$ to make $P_{havc}[i']$ a convex function of $u[i']$ over its domain without significantly change the original feasible set. In addition, $D_{SoH}[i]$ in Eqn. (23) is a convex function of $P_{bat}[i]$'s. Finally, the objective function in (25) is a convex increasing function of $P_{hvac}[i']$'s, P_{bat}'s, and $D_{SoH}[i]$. According to [24], the objective function in (25) is a convex function of all decision variables. Based on aforementioned conclusions, we know that the kernel problem can be solved efficiently using standard convex optimization tools such as CVX [25].

Because the kernel algorithm can be solved with polynomial time complexity and the outer loop can be achieved by a search algorithm (an exhaustive search in the worst case), the overall time complexity of the algorithm is pseudo-polynomial.

4. EXPERIMENTAL RESULT

4.1 Simulation Setup

In the simulations, we consider a day-ahead utility market where the time-of-use electricity prices are pre-announced at the beginning of each day, and we take one day as the billing period. The scheduling decisions of both the battery storage and the HVAC system are updated at the beginning of each hour, i.e., Δ_t is set to one hour. We adopt the electricity pricing policy from Consolidated Edison Company[1] where energy usage from 10a.m.-10p.m. is charged with a peak price, while energy usage in other hours are charged with an off-peak price.

The building temperature model as in Eqn. (19) is extracted from a building located at 1084 Columbia Ave., Irvine, California, USA. The relationship between the HVAC power consumption and the HVAC air flow in Eqn. (18) from [16] is used. The peak power of the HVAC system is set to 100kW. Because of difference in the size of the building, we use a modified set of parameters listed below:

$$c_1 = -3.8784 \times 10^{-5}, c_2 = 0.0108$$
$$c_3 = -0.48, c_4 = 59.2$$

A realistic residential PV generation system is considered, and we use PV power profiles measured at Duffield, VA, in the year 2007. The peak power generation of the PV panel is set to 20 kW. The power consumption of loads other than the HVAC ($P_{load}[i]$) is assumed to follow a uniform distribution between 5kW and 15kW. The predicted values of $\hat{P}_{pv}[i]$, $\hat{P}_{load}[i]$, and external disturbance ($\hat{D}_n[i]$) are assumed to have a maximum of $\pm 20\%$ prediction error. To model the rate capacity effect of the battery, we set factors β_c and β_d to 1.15 and 0.85, respectively. The parameters to calculate the SoH degradation as in Eqn. (13) are from [23]. The battery cost is set to \$400/kWh. The power conversion efficiencies (η_1, η_2, and η_3) are set to 90%.

4.2 Simulation Results

We first study the impact of battery storage capacity on the potential of building energy cost saving. Figure 4 shows the daily total costs (measured as the electricity bill plus the cost associated with battery aging, as described in Eqn. (15)) with different battery capacities (varying from 60kWh to 360kWh). Electricity prices in June 2014 from Consolidated Edison Company are used where the electricity price is \$0.3032/kWh during peak hours and \$0.0116 during off-peak hours. The proposed optimization framework is compared with two baseline schemes. In the first baseline scheme, the scheduling of HVAC system is performed without any available battery energy storage (marked as "No-Bat"), and in the second baseline scheme, a greedy algorithm is used to schedule the HVAC air flow and the battery charging/discharging (marked as "Greedy"). In the greedy algorithm, the battery will be charged to the maximal SoC level during off-peak hours, and discharged to the minimal SoC level during peak hours. One can observe that the proposed co-scheduling algorithm

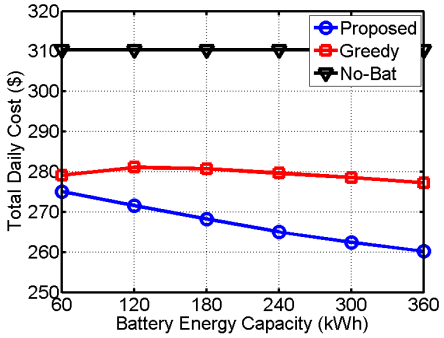

Figure 4: Relationship between daily cost and battery storage capacity for our proposed algorithm and two baseline schemes.

consistently achieves lower costs compared with both the "No-Bat" and "Greedy" schemes. Please note that the greedy algorithm can achieve a reasonable performance if the rate capacity effect and the SoH degradation of the battery do not exist because it can store a maximum amount of energy and use it in peak hours. However, it can be observed from Figure 4 that this is not the case when a realistic battery model is considered. In addition, the benefit of the proposed algorithm becomes even more significant with the increase of battery storage capacity. With a battery storage capacity of 60kWh, the proposed algorithm and the greedy algorithm achieve \$35.34/d and \$31.29/d cost saving, respectively, compared with the "No-Bat" case. When the battery energy capacity reaches 360kWh, the cost saving of the proposed algorithm achieves an increase of 43% to \$50.22/d, while the cost saving of the greedy algorithm only increases by 5.8% to \$33.14/d. The internal energy increasing rates of the battery ($P_{bat,int}$) with 180kWh of battery storage capacity are shown in Figure 5. As can be seen from this figure, large charging/discharging power is avoided in the proposed algorithm since the realistic battery model including the rate capacity effect and the SoH degradation is properly accounted for. We also conduct a study on the impact of energy prices, and Fig-

[1]http://www.coned.com/

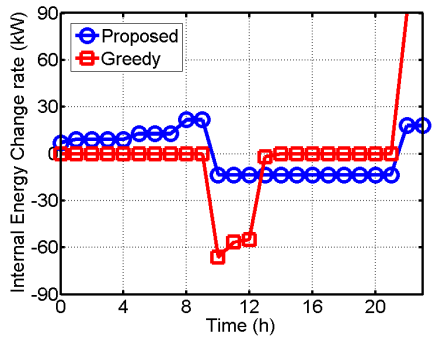

Figure 5: Battery daily charge/discharge schedule.

ure 6 shows the equivalent daily cost under different dynamic pricing functions where the electricity price during off-peak hours stays at \$0.0116/kWh while the electricity price during peak hours varies from \$0.2500/kWh to \$0.4000/kWh. The proposed algorithm also consistently achieves lower costs compared with both base line schemes with a cost reduction from 5% to 15%. The cost reduction rate stays the same with the change of peak hour energy price, indicating that the good performance of our proposed algorithm can be achieved under different dynamic pricing functions.

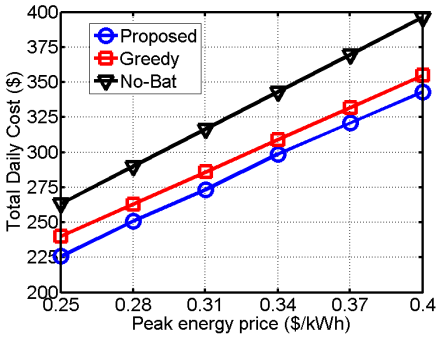

Figure 6: Relationship between daily cost and peak hour energy price for our proposed algorithm and two baseline schemes.

5. CONCLUSION

In this paper, the optimal co-scheduling problem of HVAC control and battery management is considered for energy-efficient buildings under a complete building power system and a dynamic energy pricing policy. In this problem, the degradation of battery SoH during the charging/discharging process is taken into consideration based on an accurate SoH modeling. The total cost function therefore becomes the summation of the electricity bill charged by the power grid and the extra cost associated with the aging of battery. An optimal co-scheduling algorithm is presented that adaptively adjusts its current building temperature condition and always makes the optimal building air flow control and battery charging/discharging decisions in the future time slots based on the most updated information. The proposed algorithm also accurately accounts for the power loss during the charging and discharging process of batteries, especially the rate capacity effect, and in AC-DC or DC-DC power conversion circuits, which is often neglected in the reference work. Experimental results demonstrate that the proposed optimal co-scheduling algorithm minimizes the combination of building electricity bill and battery aging cost. In our simulations, realistic data for PV energy generation and dynamic energy prices are used, and both HVAC and energy storage modeling come from actual experiments. The experimental results can serve practical purpose.

6. ACKNOWLEDGEMENT

This work is supported by the Software and Hardware Foundations program of the NSF's Directorate for Computer & Information Science & Engineering.

7. REFERENCES

[1] "Building energy data book of doe," http://buildingsdatabook.eren.doe.gov, Feb. 2012.

[2] Y. Ma, F. Borrelli, B. Hencey, B. Coffey, S. Bengea, and P. Haves, "Model predictive control for the operation of building cooling systems," *Control Systems Technology, IEEE Transactions on*, vol. 20, no. 3, pp. 796–803, 2012.

[3] M. Maasoumy, Q. Zhu, C. Li, F. Meggers, and A. Vincentelli, "Co-design of control algorithm and embedded platform for building hvac systems," in *Cyber-Physical Systems (ICCPS), 2013 ACM/IEEE International Conference on*. IEEE, pp. 61–70.

[4] M. Maasoumy and A. Sangiovanni-Vincentelli, "Total and peak energy consumption minimization of building hvac systems using model predictive control," *IEEE Design & Test of Computers*, vol. 29, no. 4, 2012.

[5] T. Wei, T. Kim, S. Park, Q. Zhu, S. X.-D. Tan, N. Chang, S. Ula, and M. Maasoumy, "Battery management and application for energy-efficient buildings," in *Design Automation Conference (DAC), 2014 51st ACM/EDAC/IEEE*. IEEE, 2014, pp. 1–6.

[6] J. Tu, L. Lu, M. Chen, and R. K. Sitaraman, "Dynamic provisioning in next-generation data centers with on-site power production," in *Proceedings of the fourth international conference on Future energy systems*. ACM, 2013, pp. 137–148.

[7] J. A. Muckstadt and R. C. Wilson, "An application of mixed-integer programming duality to scheduling thermal generating systems," *Power Apparatus and Systems, IEEE Transactions on*, no. 12, 1968.

[8] M. Chen and G. A. Rincon-Mora, "Accurate electrical battery model capable of predicting runtime and iv performance," *Energy conversion, ieee transactions on*, vol. 21, no. 2, pp. 504–511, 2006.

[9] T. Cui, Y. Wang, S. Chen, Q. Zhu, S. Nazarian, and M. Pedram, "Optimal control of pevs for energy cost minimization and frequency regulation in the smart grid accounting for battery state-of-health degradation," in *Proceedings of the 52nd Annual Design Automation Conference*. ACM, 2015, p. 134.

[10] A. Ipakchi and F. Albuyeh, "Grid of the future," *Power and Energy Magazine, IEEE*, vol. 7, no. 2, pp. 52–62, 2009.

[11] K. Shimizu, T. Masuta, Y. Ota, and A. Yokoyama, "Load frequency control in power system using vehicle-to-grid system considering the customer convenience of electric vehicles," in *Power System Technology (POWERCON), 2010 International Conference on*. IEEE, 2010, pp. 1–8.

[12] "Renewable 2013 global status report (gsr)," http://www.ren21.net/ren21activities/globalstatusreport.aspx.

[13] C. O. Adika and L. Wang, "Autonomous appliance scheduling for household energy management," *Smart Grid, IEEE Transactions on*, vol. 5, no. 2, pp. 673–682, 2014.

[14] J. Li, Y. Wang, T. Cui, S. Nazarian, and M. Pedram, "Negotiation-based task scheduling to minimize user's electricity bills under dynamic energy prices," in *Green Communications (OnlineGreencomm), 2014 IEEE Online Conference on*, Nov 2014, pp. 1–6.

[15] J. Li, Y. Wang, X. Lin, S. Nazarian, and M. Pedram, "Negotiation-based task scheduling and storage control algorithm to minimize user's electric bills under dynamic prices," in *Design Automation Conference (ASP-DAC), 2015 20th Asia and South Pacific*. IEEE, 2015, pp. 261–266.

[16] M. Maasoumy, C. Rosenberg, A. Sangiovanni-Vincentelli, and D. S. Callaway, "Model predictive control approach to online computation of demand-side flexibility of commercial buildings hvac systems for supply following," in *American Control Conference (ACC), 2014*. IEEE, 2014, pp. 1082–1089.

[17] D. Linden and T. Reddy, "Handbook of batteries, 2002."

[18] W. Peukert, "An equation for relating capacity to discharge rate," *Electrotech, Z.*, vol. 18, p. 287, 1897.

[19] Y. Wang, X. Lin, Q. Xie, N. Chang, and M. Pedram, "Minimizing state-of-health degradation in hybrid electrical energy storage systems with arbitrary source and load profiles," in *Design, Automation and Test in Europe Conference and Exhibition (DATE), 2014*. IEEE, 2014, pp. 1–4.

[20] M. Dubarry, V. Svoboda, R. Hwu, and B. Y. Liaw, "Capacity and power fading mechanism identification from a commercial cell evaluation," *JPS*, vol. 165, no. 2, pp. 566–572, 2007.

[21] S. B. Peterson, J. Apt, and J. Whitacre, "Lithium-ion battery cell degradation resulting from realistic vehicle and vehicle-to-grid utilization," *Journal of Power Sources*, vol. 195, no. 8, pp. 2385–2392, 2010.

[22] Q. Zhang and R. E. White, "Capacity fade analysis of a lithium ion cell," *Journal of Power Sources*, vol. 179, no. 2, pp. 793–798, 2008.

[23] A. Millner, "Modeling lithium ion battery degradation in electric vehicles," in *Innovative Technologies for an Efficient and Reliable Electricity Supply (CITRES), 2010 IEEE Conference on*. IEEE, 2010, pp. 349–356.

[24] S. Boyd and L. Vandenberghe, *Convex optimization*. Cambridge university press, 2009.

[25] M. Grant and S. Boyd, "CVX: Matlab software for disciplined convex programming, version 2.1," http://cvxr.com/cvx, Mar. 2014.